Fall 9-1-1986

Effects of Cover-Layer on Radiation and Surface Waves of a Microstrip Patch Antenna

Ahmad Hoorfar
University of Colorado Boulder

K C. Gupta
University of Colorado Boulder

David C. Chang
University of Colorado Boulder

SCIENTIFIC REPORT NO. 88

EFFECTS OF COVER-LAYER ON RADIATION AND SURFACE WAVES OF A MICROSTRIP PATCH ANTENNA

Ahmad Hoorfar, K.C. Gupta, and D.C. Chang

Electromagnetics Laboratory
Department of Electrical and Computer Engineering
Campus Box 425
University of Colorado
Boulder, Colorado

September 1986

This work has been supported by the Department of the Navy
under Contract # NAVYN6053084.COO95

EFFECTS OF COVER-LAYER ON RADIATION AND SURFACE WAVES OF A MICROSTRIP PATCH ANTENNA

Abstract

The effects of a thick cover-layer on the radiation pattern, surface-wave modes and efficiency of a microstrip-patch antenna are investigated. Assuming a very thin substrate, the patch is modeled with a magnetic line source on a conducting plane with a possibly thick dielectric cover of thickness, t. This model is used to calculate the radiation pattern as well as the radiated and surface-wave power as a function of cover-layer thickness, k_0t. It is found that the beamwidth in E-plane will initially decrease and then increase upon increasing k_0t. It is also shown that for the values of $k_0t \gtrsim 1$, the power carried by the surface-waves is almost entirely contained inside the cover-layer; this suggests the possibility of placing a graded lossy thin-film between the substrate and the cover layer in order to attenuate the surface-waves propagation (and their eventual radiation as a side lobe). Numerical results are presented to show the effects of a lossy dielectric cover-layer on the surface-waves and the radiated power.

Table of Contents

List of Figures

1. Introduction

The conductive patches of microstrip antennas are often covered by a dielectric layer for protective purposes, or other mechanical/thermal requirements. In many of these practical designs, this cover-layer (or superstrate) is electrically much thicker than the substrate thickness, and can adversely affect the antenna basic radiation characteristics. In particular, due to the relatively strong excitation of the surface-waves in the cover-layer, the antenna radiation efficiency can become rather low; also for a finite-sized cover-layer, the diffraction of surface-waves from the edges may result in spurious radiation, and undesirable effects on side lobe level and polarization characteristics.

The basic properties of microstrip antennas with a cover-layer are discussed in [1], by solving the problem of a Hertzian electric dipole. It is well known, however, that the equivalent aperture or magnetic current method presents a simpler and a more accurate model for evaluating the radiation properties of the microstrip patch antennas [2,3]. In this report, we formulate the problem of cover layer effects based on a magnetic current model.

In order to assess the effect of a dielectric cover-layer, the problem of a grounded dielectric slab with a truncated upper conductor is considered (Figure 1). Assuming a very thin substrate thickness, d, the patch antenna is then modeled by a magnetic line source of intensity P_m (volts) on a conducting ground plane with a possibly thick dielectric cover-layer, t. As it is well known, the equivalent magnetic current strength P_m at the slot can be approximately obtained from the z-directed electric field inside the parallel-plates region using the Hyugen's principle [2,4], provided that $k_1 d \ll k_1 t$. This model (Figure 1-b) is used in sections 2, 3 and 4 to formulate the (space-wave) radiation fields and radiated power as well as the surface-wave power of the patch antenna with a dielectric cover-layer. In section 5, numerical results are presented to

show the effects of the cover-layer thickness on radiation pattern and efficiency of the antenna. The effects of a lossy dielectric on the surface-waves and the radiated power are also discussed. In particular, it is shown that a graded loss could be used to substantially reduce the surface-wave "side-lobe" radiation.

2. Formulation of the Problem

Let us consider a magnetic current line source, $\bar{J}_m$, which is placed on a perfectly conducting ground plane and is covered with a dielectric-layer of thickness t (Figure 1-b). The line source has a strength of P_m (volts) and is assumed to be extended infinitely in the x-direction. As shown in Figure 1, the permittivities in the air and the cover-layer regions are ϵ_0 and ϵ_1, respectively; the permeability in both media is assumed to be μ_0.

Because there are no variations in the fields with respect to x, the corresponding TM_z fields can be written as [5]:

$$E_y = \frac{\partial}{\partial y}\left(\frac{\partial \Pi_e}{\partial z}\right) \quad , \quad E_z = -\frac{\partial^2 \Pi_e}{\partial y^2} \tag{1}$$

$$H_x = -i\omega\epsilon \frac{\partial \Pi_e}{\partial_y}$$

where Π_e is the z component of electric Hertz vector potential; $\epsilon = \epsilon_0$ or ϵ depending upon the medium in which the observation point is located. The time dependence $e^{-i\omega t}$ is being suppressed throughout this paper. The boundary conditions may be written in terms of conditions for E_z, as:

$$\frac{\partial E_z}{\partial z} = -\frac{\partial J_m}{\partial y} \tag{2.1}$$

at z = 0, and

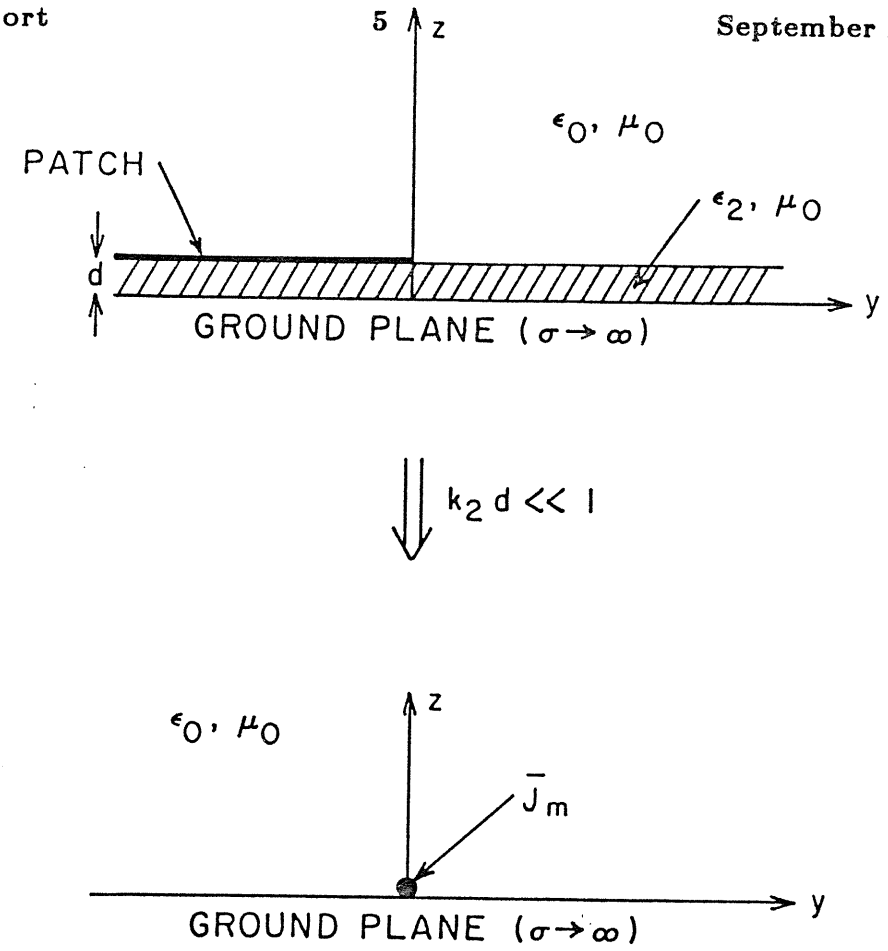

Fig. 1-a: Model of a radiating-edge of a thin microstrip patch antenna without a cover-layer.

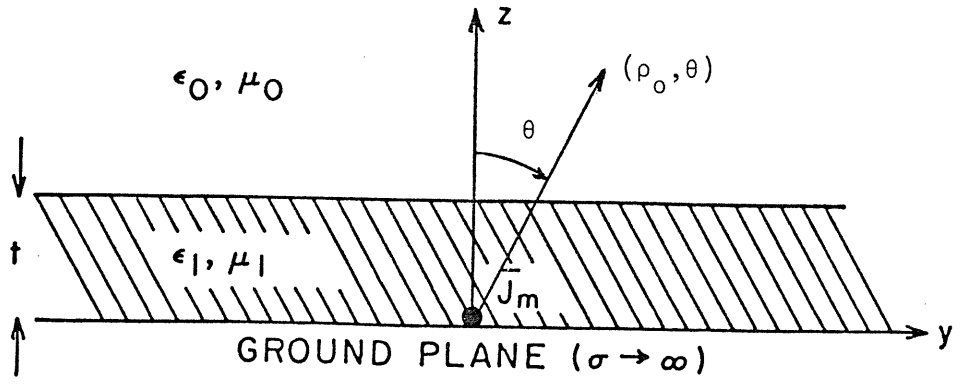

Fig. 1-b: The model for a thin microstrip patch antenna with a cover-layer.

$$E_z|_{z_+} = \epsilon_r E_z|_{z_-} \quad ; \quad \frac{\partial E_z}{\partial z}|_{z_+} = \frac{\partial E_z}{\partial z}|_{z_-} \tag{2.2}$$

at $z = t$, where $\epsilon_r = (\epsilon_1/\epsilon_0)$ is the refractive index of the cover-layer.

Defining the Fourier transform pair as,

$$\Pi_e(y) = \int_{-\infty}^{\infty} \tilde{\Pi}_e(\beta) e^{+ik_0\beta y}\, d\beta \tag{3.1}$$

$$\tilde{\Pi}_e(\beta) = \left(\frac{k_0}{2\pi}\right) \int_{-\infty}^{\infty} \Pi_e(y)\, e^{-ik_0\beta y}\, dy \tag{3.2}$$

the potential $\tilde{\Pi}_e$ now satisfies the equation

$$\left(\frac{\partial^2}{\partial z^2} - k_0^2 U_{0,1}\right) \tilde{\Pi}_e = 0 \qquad z \neq 0 \tag{4}$$

where

$$U_0 = \sqrt{\beta^2 - 1} \quad , \quad U_1 = \sqrt{\beta^2 - \epsilon_r}$$
$$\mathrm{Re}(U_{0,1}) > 0 \quad , \quad \mathrm{Im}(U_{0,1}) < 0 \tag{5}$$

the solution of Eq. 4, subject to the boundary conditions in (2), is found to be

$$\tilde{\Pi}_e = E_1[\mathrm{sh}(U_1 k_0 z) + \Gamma_e \,\mathrm{ch}(U_1 k_0 z)] \quad ; \quad 0 < z < t \tag{6}$$

$$\tilde{\Pi}_e = E_0\, e^{-U_0 k_0 (z - t)} \quad ; \quad z > t \tag{7}$$

where

$$E_0 = \left(\widetilde{\frac{\partial J_m}{\partial y}}\right) \frac{\epsilon_r}{k_0^3 \beta^2} \cdot \frac{1}{\mathrm{ch}(U_1 k_0 t) D_{TM}} \tag{8}$$

$$E_1 = - \left(\frac{\widetilde{\partial J_m}}{\partial y}\right) \frac{1}{k_0^3 \beta^2 U_1} \tag{9}$$

$$\Gamma_e = - \frac{1}{D_{TM}} [U_1 + \epsilon_r U_0 th(U_1 k_0 t)] \tag{10}$$

wherein

$$D_{TM} = \epsilon_r U_0 + U_1 th(U_1 k_0 t) \tag{11}$$

For the present case of the magnetic line source, i.e., $J_m = P_m \delta(y)\delta(z)$, we have

$$\widetilde{\frac{\partial J_m}{\partial y}} = \left(\frac{k_0^2}{2\pi} P_m\right) \beta \tag{12}$$

Equations (6) and (7), via (3.1), now yield the formal expression for Π_e as

$$\Pi_e = \left(\frac{- iP_m}{2\pi k_0}\right) \int_{-\infty}^{\infty} \beta \, \tilde{f}_e(U_0) e^{- k_0 U_0 z + i k_0 \beta y} \frac{d\beta}{U_0} \tag{13}$$

where

$$\tilde{f}_e(U_0) = \frac{U_0}{(1 + U_0^2)U_1} [sh(U_1 k_0 z) + \Gamma_e \, ch(U_1 k_0 z)] \, e^{k_0 U_0 z} \tag{14}$$

for $0 < z < t$, and

$$\tilde{f}_e(U_0) = \left(\frac{\epsilon_r U_0}{1 + U_0^2}\right) \frac{e^{+ U_0 k_0 t}}{ch(U_1 k_0 t) D_{TM}} \tag{15}$$

for $z > t$, wherein $U_1 = \sqrt{U_0^2 + 1 - \epsilon_r}$.

3. Far-Field Approximation

3.1 Space-Wave Radiation

For the two-dimensional free-space Green's function, we have the well-known identity:

$$\int_{-\infty}^{\infty} e^{-k_0 U_0 |z - z'| + ik_0\beta(y - y')} \frac{d\beta}{U_0} = i\pi H_0^{(1)}(k_0\rho) \tag{16}$$

$$\simeq i\pi \sqrt{\frac{2}{\pi k_0 \rho}}\, e^{i(k_0\rho - \frac{\pi}{4})} \quad ; \quad k_0\rho > > 1$$

where

$$\rho = [(y - y')^2 + (z - z')^2]^{1/2}$$

Since for $(y',z') < < |\bar{\rho}_0|$ one has

$$\rho \simeq \rho_0 - y'\sin\theta - z'\cos\theta \quad ; \quad \rho_0 = \sqrt{y^2 + z^2}$$

therefore, in general one can write for $(k_0 y, k_0 z) > > 1$,

$$\int_{-\infty}^{\infty} \tilde{f}(\beta, U_0)\, e^{-U_0 k_0 z + ik_0\beta y} \frac{d\beta}{U_0} \simeq i\sqrt{2\pi}\, \tilde{f}(\sin\theta \; ; \; -i\cos\theta) \frac{e^{i(k_0\rho_0 - \frac{\pi}{4})}}{\sqrt{k_0\rho_0}} \tag{17}$$

The result in (17) can also be obtained directly from the stationary-phase method [6]. Far-field patterns of Π_e are derived by applying (17) to the integral in (13), for $z > t$,

$$\Pi_e \simeq \frac{P_m}{k_0} \cdot \frac{e^{i(k_0\rho_0 - \frac{\pi}{4})}}{\sqrt{2\pi k_0 \rho_0}} \sin\theta \tilde{f}_e(-i\cos\theta) \tag{18}$$

where $\tilde{f}_e$ is given by (15).

The far-field expressions for the electric and magnetic fields (i.e., the space-wave fields) can be obtained by inserting (18) into (1). By keeping the $\left(\frac{1}{\rho_0}\right)^{1/2}$ terms only, the space-wave radiated fields, in cylindrical coordinates (ρ_0,θ,x), are given by

$$\begin{cases} E_\theta(\rho,\theta) \simeq -k_0 P_m \dfrac{e^{i(k_0\rho_0 - \frac{\pi}{4})}}{\sqrt{2\pi k_0\rho_0}} \sin^2\theta \, \tilde{f}_e(-i\cos\theta) \\ H_x(\rho,\theta) = -\dfrac{1}{\eta_0} E_\theta(\rho,\theta) \quad ; \quad \eta_0 = 120\pi \end{cases} \tag{19}$$

or by substituting for $\tilde{f}_e$ from (15) into (19),

$$E_\theta(\rho,\theta) \simeq iP_m \epsilon_r k_0 \frac{e^{i(k_0\rho_0 - \frac{\pi}{4})}}{\sqrt{2\pi k_0\rho_0}} \cdot \frac{e^{-ik_0 t\cos\theta}}{\cos(k_\theta t) D^\theta_{TM}} \cos\theta \tag{20}$$

where

$$\begin{aligned} D^\theta_{TM} &= -i\epsilon_r\cos\theta - \sqrt{\epsilon_r - \sin^2\theta}\,\tan(k_\theta t) \\ k_\theta &= k_0\sqrt{\epsilon_r - \sin^2\theta} \end{aligned} \tag{21}$$

3.2 Radiated Power, Radiation Conductance and Directivity

The (space-wave) radiated power per unit length of the magnetic line source (Figure 1b) can be written as

$$P_r = \int_{-\frac{\pi}{2}}^{\frac{\pi}{2}} S(\theta)\rho_0 \, d\theta$$

where

$$S(\theta) = \frac{1}{2\eta_0} |E_\theta|^2 \tag{22}$$

is the power density in space. By inserting for E_θ from (20) into (22), we have

$$P_r = P_0 Q_t \tag{23}$$

where

$$P_0 = \frac{k_0 P_m^2}{4\eta_0} \tag{24}$$

and

$$Q_t = \int_0^1 |\hat{f}_e(\frac{\pi}{2}\alpha)|^2 \cos^2(\frac{\pi}{2}\alpha)\, d\alpha \tag{25}$$

wherein

$$|\hat{f}_e(\theta)|^2 = \frac{\epsilon_r^2}{\cos^2(k_\theta t)} \cdot \frac{1}{\epsilon_r^2 \cos^2\theta + (\epsilon_r - \sin^2\theta)\tan^2(k_\theta t)} \tag{26}$$

In (24), P_0 is the power radiated by a magnetic line source over a perfectly-conducting ground in the absence of any cover-layer. We note that in the latter case, i.e., $t = 0$, the value of the integral in (25) is one, and therefore a dielectric cover (i.e., $t > 0$) will effect the radiated power explicitly through the value of this integral, which in general has to be evaluated numerically.

The radiation conductance per unit length can be defined from

$$P_r = \frac{1}{2} P_m^2 G_r$$

After simplification,

$$G_r = \frac{k_0}{2\eta_0} Q_t \tag{26}$$

Finally, the directivity of the line source is given by

$$D = \frac{(2\pi\rho_0)S(0)}{P_r}$$

which simplifies to

$$D = \frac{2}{\cos^2(k_1 t)\left[1 + \frac{1}{\epsilon_r}\tan^2(k_1 t)\right]} \cdot \frac{1}{Q_t} \tag{27}$$

where $k_1 = \sqrt{\epsilon_r}\, k_0$, and Q_t is given by (25).

4. Surface-Wave Power and Radiation Efficiency

The complex β-plane for the integrand in (13) is shown in Figure 2. An integration along the branch-cut, which is defined by $\mathrm{Re}(U_0) \geq 0$, yields the continuous spectrum, while a residue calculation at the surface-wave pole, β_ρ, $p = 1, 2, 3, \ldots N_{max}$, gives the discrete part of the spectrum. The TM surface-wave pole β_ρ are the zeroes of D_{TM} in (11), i.e.,

$$D_{TM}(\beta_\rho) = \epsilon_r \sqrt{\beta_\rho^2 - 1} - \sqrt{\epsilon_r - \beta_\rho^2}\tan\left(k_0 t \sqrt{\epsilon_r - \beta_\rho^2}\right) = 0 \tag{28}$$

The maximum number of the poles ($1 < \beta_\rho < \sqrt{\epsilon_r}$) is given by [6]

$$N_{max} < \frac{\Delta}{\pi} + 1 \quad ; \quad \Delta = k_0 t\sqrt{\epsilon_r - 1} \tag{29}$$

We note that for $0 < z < t$, the first term in (14) does not have any poles, therefore, the surface-wave mode contribution to Π_e can be written as

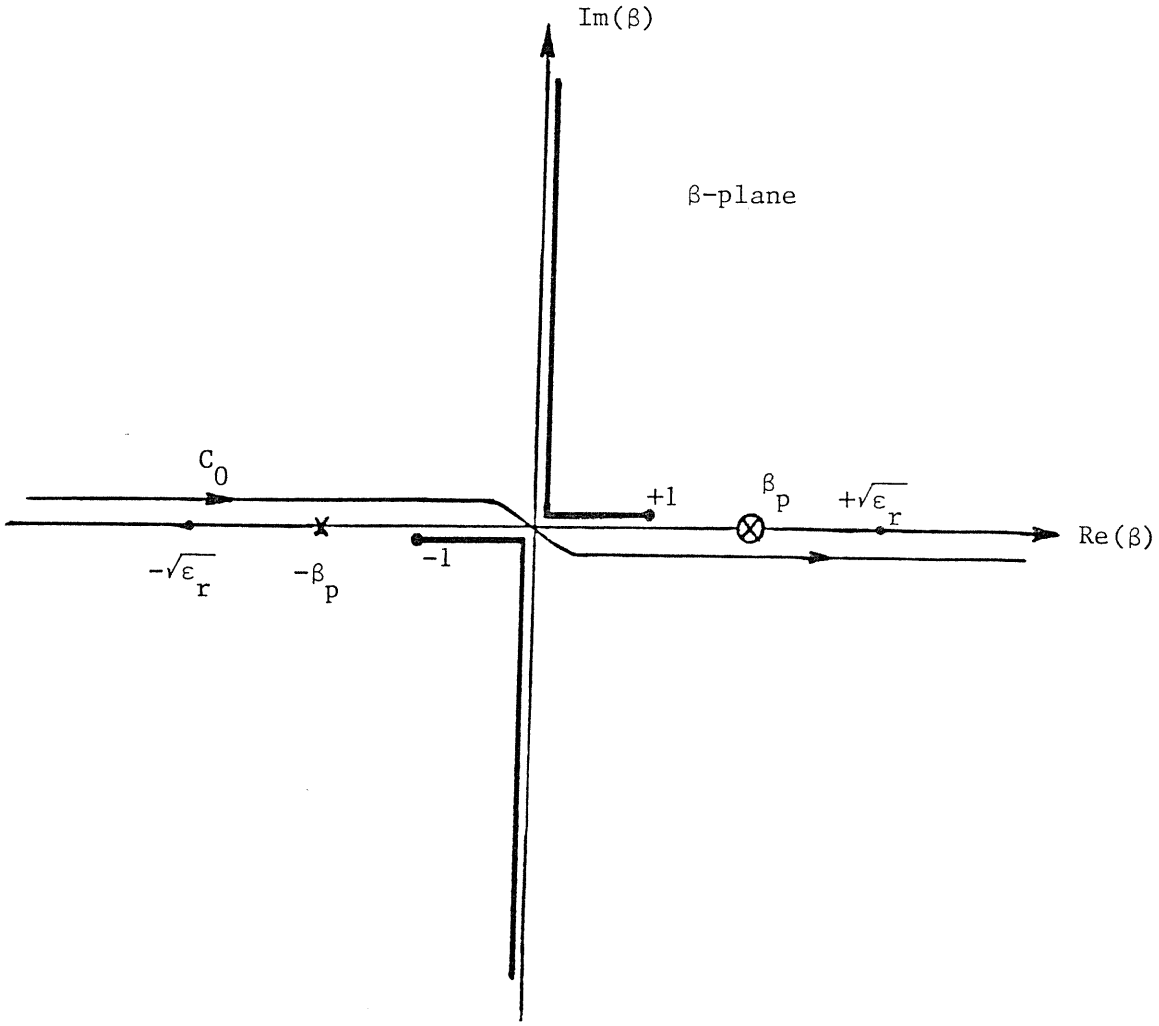

Fig. 2: The complex β-plane.

$$\Pi_{SW} = \frac{P_m}{k_0} \sum_{\rho} \frac{1}{\beta_\rho D'_{TM}(\beta_\rho)} g_1(\beta_\rho) \cos(\lambda_\rho k_0 z)\, e^{ik_0\beta_\rho y} \qquad \textbf{(30.1)}$$

for $0 < z < t$, and

$$\Pi_{SW} = \frac{P_m}{k_0} \sum_{p} \frac{1}{\beta_p D'_{TM}(\beta_p)} g_2(\beta_p)\, e^{-U_{0p}k_0 z}\, e^{ik_0\beta_p y} \qquad (30.2)$$

for $z > t$, where

$$g_1(\beta_\rho) = -\frac{1}{\lambda_\rho}\left[\lambda_\rho + \epsilon_r U_{0\rho} \tan(k_0\lambda_\rho t)\right] \qquad (31.1)$$

$$g_2(\beta_\rho) = \frac{\epsilon_r}{\cos(k_0\lambda_\rho t)}\, e^{-U_{0\rho}k_0 t} \qquad (31.2)$$

and

$$D'_{TM}(\beta_\rho) = \frac{\partial D_{TM}}{\partial \beta}\Big|_{\beta=\beta_\rho} = \beta_\rho \left[\frac{\epsilon_r}{U_{0\rho}} + \frac{1}{\lambda_\rho}\tan(k_0\lambda_\rho t) + \frac{k_0 t}{\cos^2(k_0\lambda_\rho t)}\right] \qquad (32)$$

wherein

$$U_{0\rho} = \sqrt{\beta_\rho^2 - 1} \quad ; \quad \lambda_\rho = \sqrt{\epsilon_r - \beta_\rho^2}$$

Now the (time-average) surface-wave power per unit length is given by

$$P_{SW} = \frac{1}{2}\,\mathrm{Re}\int_0^\infty (E_z H_x^*)_{SW}\, dz \qquad (33)$$

By substituting for $(E_z)_{SW}$ and $(H_x)_{SW}$ from (1) and (30) and then integrating (33) in the intervals, (0,t) and (t,∞), we finally arrive at the following expression for the total surface-wave power

$$P_{SW} = P_{SW}^{(1)} + P_{SW}^{(2)} \qquad (34)$$

where

$$P_{SW}^{(1)} = \epsilon_r P_0 \sum_{\rho} \beta_\rho G_1(\beta_\rho) \left[k_0 t + \frac{1}{2\lambda_\rho} \sin(2k_0 \lambda_\rho t) \right] \tag{35}$$

$$P_{SW}^{(2)} = P_0 \sum_{\rho} \frac{\beta_\rho}{U_{0\rho}} G_2(\beta_\rho) e^{-2U_{0\rho} k_0 t} \tag{36}$$

wherein $P_0 = \frac{k_0 P_m^2}{4\eta_0}$ and

$$G_{1,2}(\beta_\rho) = \frac{|g_{1,2}(\beta_\rho)|^2}{|D_{TM}'(\beta_\rho)|^2} \tag{37}$$

In deriving (34-36), the orthogonality property of the surface-wave modes is used. We note that $P_{SW}^{(1)}$ and $P_{SW}^{(2)}$ are the powers carried by the surface-wave modes inside ($0 < z < t$) and outside ($z > t$) of the cover-layer, respectively.

The expressions given in (35) and (36) are obtained by assuming dielectric cover-layer to be lossless. For the case of a lossy dielectric with $\epsilon_r' = \epsilon_r(1 + i\tan\delta)$, the surface-wave mode, β_ρ, is complex and (35-36) should be modified as

$$P_{SW}^{(1)} = P_0 \sum_{\rho} \mathrm{Re}\left(\frac{\epsilon_r'}{\beta_\rho}\right) |\beta_\rho|^2 G_1(\beta_\rho) \left[\frac{1}{2\lambda_{\rho r}} \sin(2k_0 \lambda_{\rho r} t) + \frac{1}{2\lambda_{\rho i}} \mathrm{sh}(2k_0 \lambda_{\rho i} t) \right] e^{-2k_0 \beta_{\rho i} y} \tag{38}$$

$$P_{SW}^{(2)} = P_0 \sum_{\rho} \frac{\mathrm{Re}(\frac{1}{\beta_\rho})}{U_{0r}} |\beta_\rho|^2 G_2(\beta_\rho) e^{-2U_{0r} k_0 t} e^{-2k_0 \beta_{\rho i} y} \tag{39}$$

where

$$\beta_{\rho i} = \mathrm{Im}(\beta_\rho) \quad ; \quad U_{0r} = \mathrm{Re}(U_{0\rho})$$

$$\lambda_{\rho r} = \mathrm{Re}(\lambda_\rho) \quad ; \quad \lambda_{\rho i} = \mathrm{Im}(\lambda_\rho)$$

and G_1 and G_2 are given in (37) with $\epsilon_r \to \epsilon_r'$.

The maximum number of TM surface-wave modes supported by the cover-layer structure is given by (29). We note that for typical values of $\epsilon_r = 2.5$ and $k_0 t \leq 2.5$ we have $N_{max} = 1$, i.e., only TM_0 mode is excited; in this case the summation in (35-36) and (38-39) will be reduced to a single term corresponding to the first TM mode (i.e., TM_0 mode).

Neglecting dielectric losses, the antenna radiation efficiency is now defined as the ratio of radiated power to total (radiated plus surface wave) power,

$$e_s = \frac{P_r}{P_r + P_{SW}} \tag{40}$$

Both P_r and P_{SW} are proportional to P_0, and hence the result is independent of the magnetic-current strength P_m. It can be shown that, for $k_0 t << 1$,

$$P_{SW} \simeq P_0 \left(\frac{\epsilon_r - 1}{\epsilon_r}\right) k_0 t \tag{41}$$

$$e_s \simeq 1 - \left(\frac{\epsilon_r - 1}{\epsilon_r}\right) k_0 t \tag{42}$$

The wall or edge conductance of the patch can now be expressed as the total, radiation plus surface-wave, conductance (per unit length) of the magnetic line source,

$$G_W = G_r + G_{SW} \tag{43}$$

$$= \frac{k_0}{2\eta_0} Q_t + \frac{2}{P_m^2} P_{SW}$$

where Q_t and P_{SW} are given in (25) and (34), respectively. When no cover-layer is present, we have $G_w^0 = \frac{k_0}{2\eta_0}$, which is identical to the conductance of an electrically small (waveguide) slot radiating into a half-space [5]. It is noteworthy that G_w^0 is often

used as an approximation to the wall conductance (per unit length) of the "radiating edges", in the design of microstrip patch antennas with electrically thin substrate [7].

5. Numerical Results

5.1 Loss-Less Cover-Layer

By using Eq. (20), the radiation pattern of $|E_\theta|$ is calculated and plotted in Figures 3, 4 and 5, for $\epsilon_r = 2.5$ and for various values of cover thickness k_0t. We note that the 3 dB beamwidth in E-plane reduces when k_0t is increased to 1.0, increases again when k_0t is varied from 1.0 to 2.0 and decreases again with further increase in k_0t.

Figure 6 shows the radiated power, P_r and the (TM_0) surface-wave power P_{SW} as a function of k_0t and for $\epsilon_r = 2.5$. Also included in this figure are the two components of the surface-wave power, i.e., $P_{SW}^{(1)}$ and $P_{SW}^{(2)}$. The powers are normalized to P_0, which is the radiated power due to a magnetic line-source when no cover-layer is present, i.e., $k_0t = 0$. As can be seen, the radiated power P_r has a peak value near $k_0t \simeq 1.0$. Because of the sharp increase in the value of P_{SW} near $k_0t = 1.0$, however, this maximum does not translate to a peak in the value of radiation efficiency given by (40). In fact as shown in Figure 7, the efficiency is less than 70% for $k_0t \gtrsim 1.0$. Also this figure confirms that for $k_0t < < 1$, e_s behaves like the approximate expression in (42).

It is noteworthy that for $k_0t < 0.5$, the major contribution to P_{SW} comes from $P_{SW}^{(2)}$, which is the power carried by the surface-wave outside the cover-layer, whereas for $k_0t \gtrsim 1.0$, the total surface-wave power P_{SW} is almost entirely given by $P_{SW}^{(1)}$, i.e., the power carried by the surface-wave inside the cover-layer. This phenomenon suggests the possibility of using a thin-layer of lossy material between the substrate and the cover-layer in order to attenuate the surface-wave propagation for thicknesses of $k_0t \simeq 1.0$ and greater.

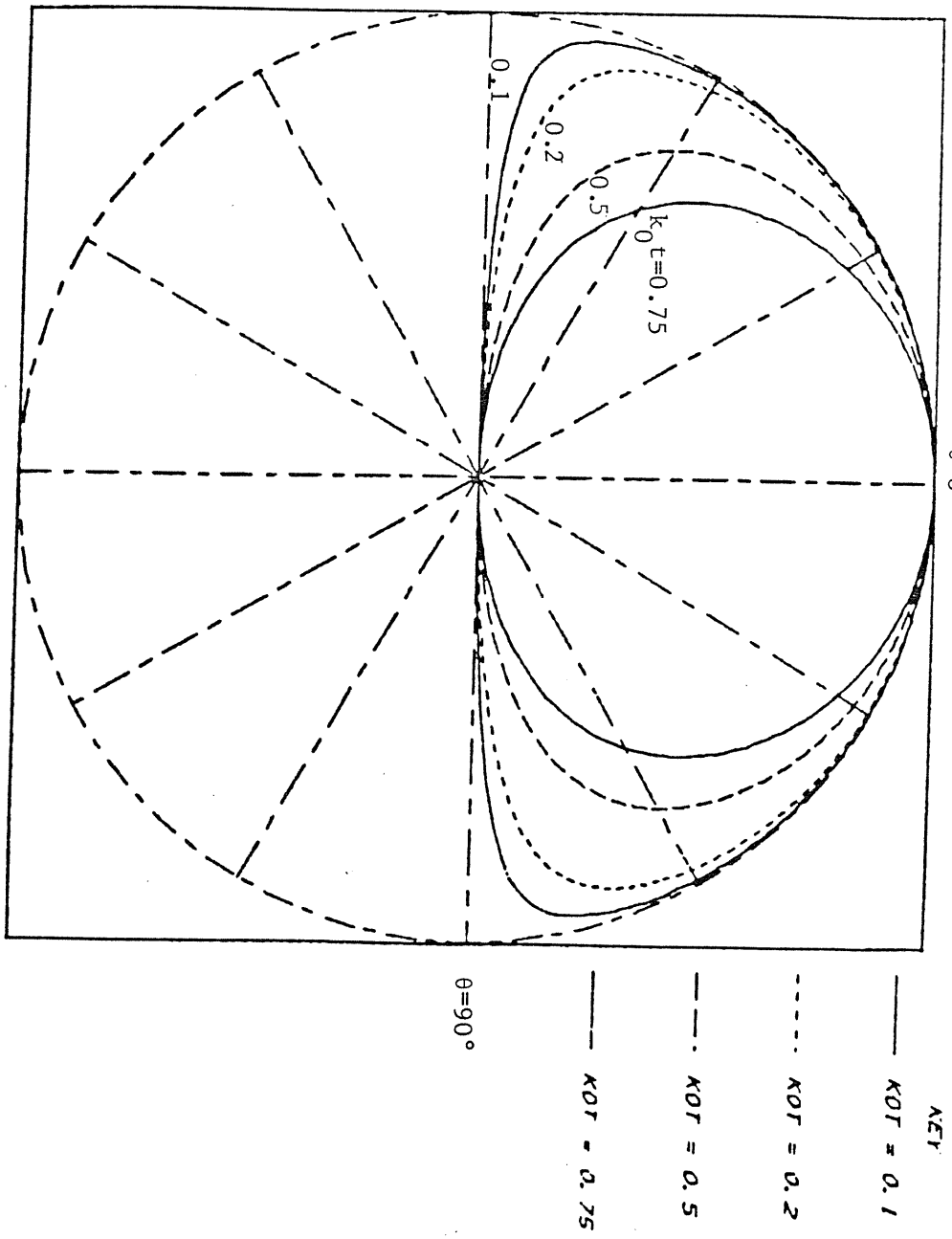

Fig. 3: The radiation pattern, $|E_\theta|$, for various values of the cover-layer thickness, k_0t = 0.1, 0.2, 0.5 and 0.75; ε_r = 2.5.

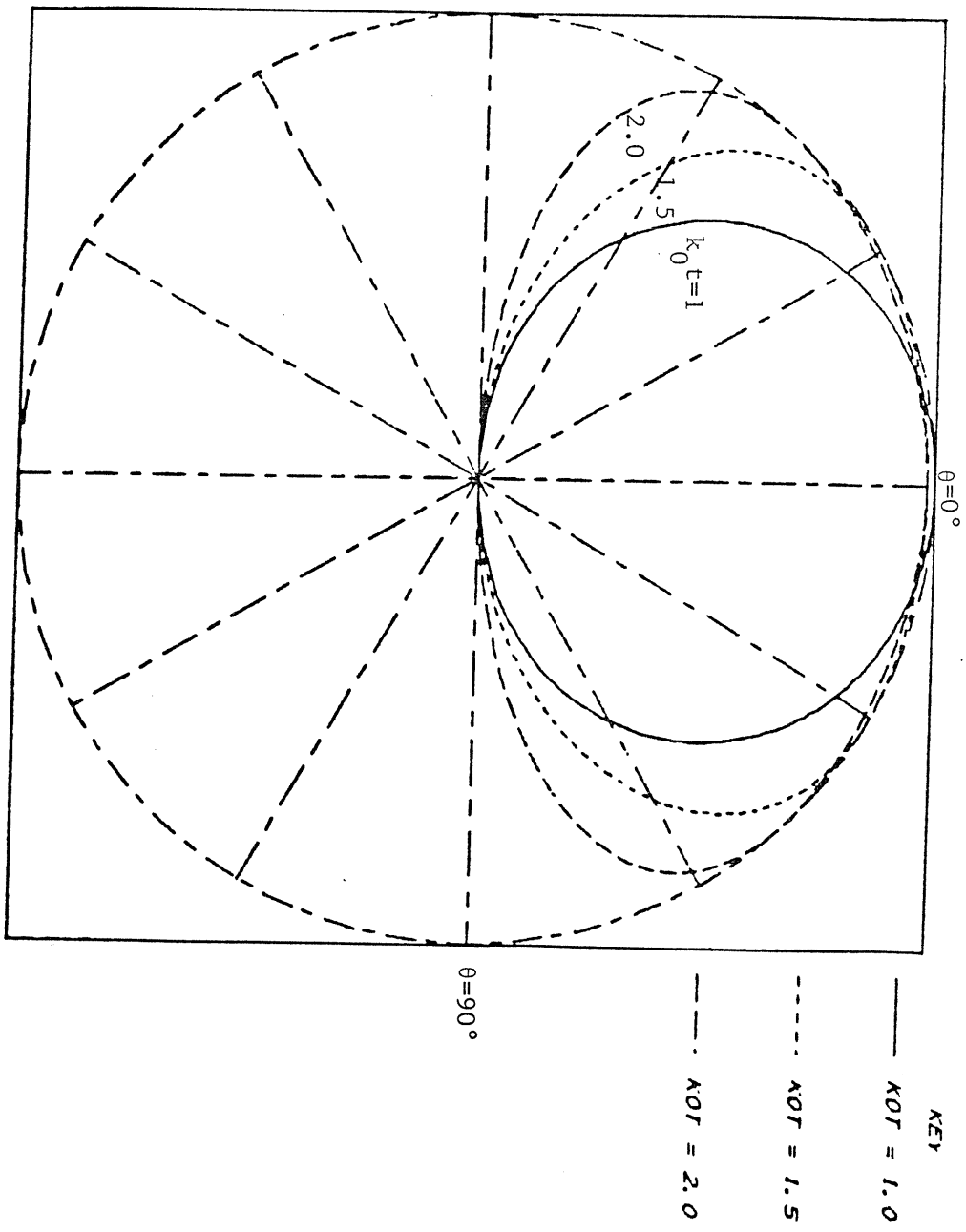

Fig. 4: The radiation pattern, $|E_\theta|$, for various values of the cover-layer thickness, k_0t = 1.0, 1.5 and 2.0; ε_r = 2.5.

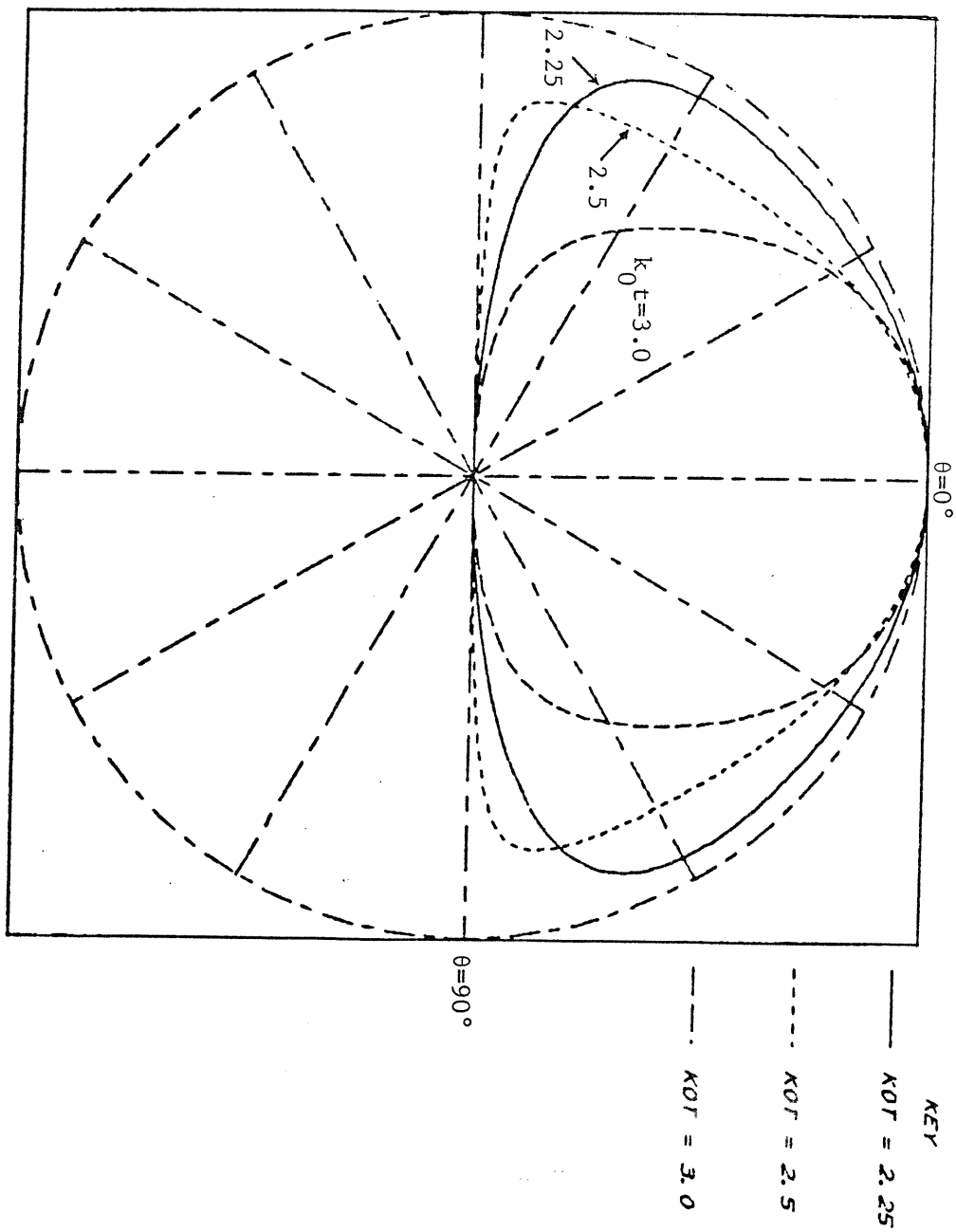

Fig. 5: The radiation pattern, $|E_\theta|$, for various values of the cover-layer thickness, k_0t = 2.25, 2.5 and 3.0; ε_r = 2.5.

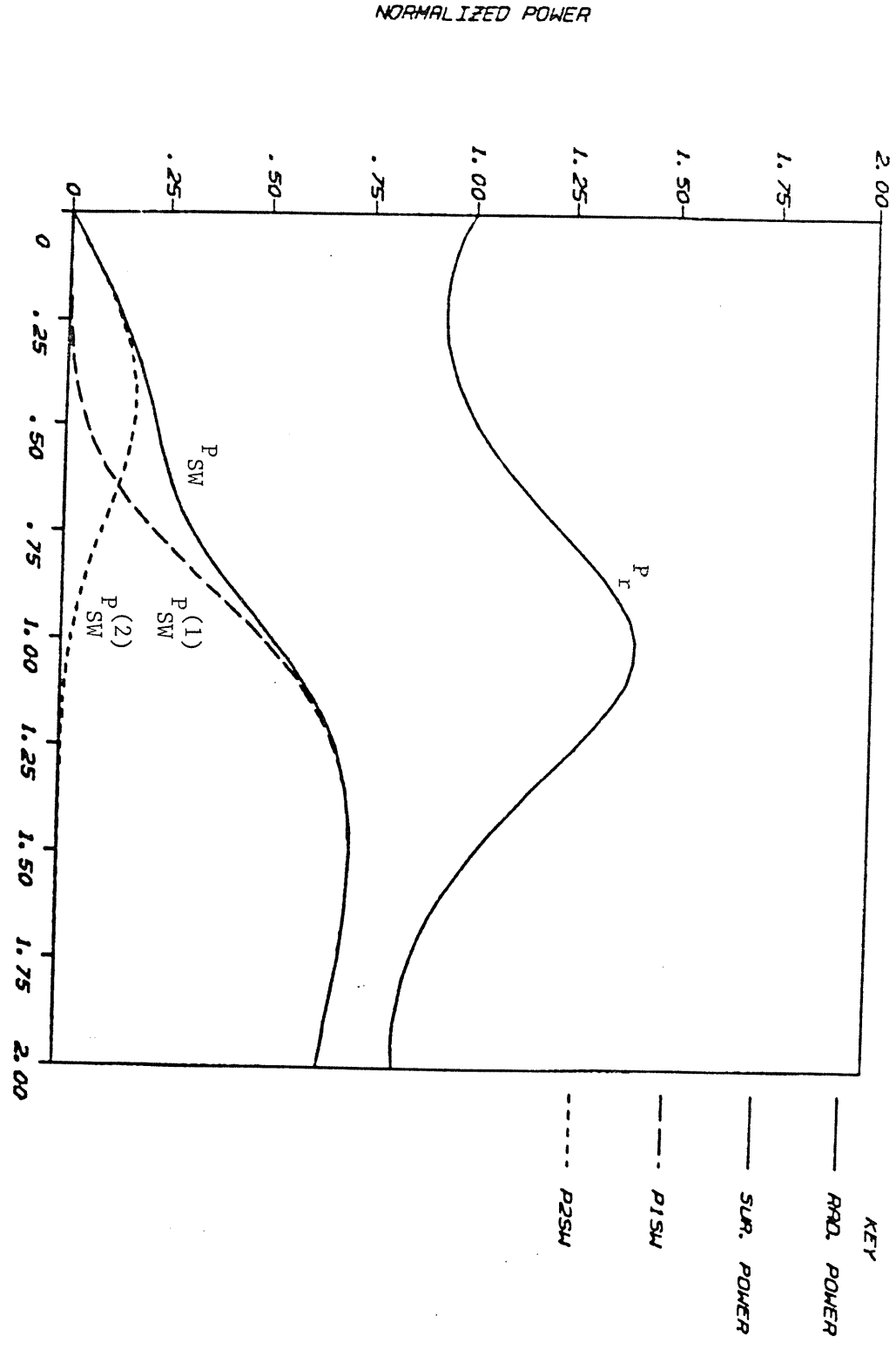

Fig. 6: The normalized radiated and surface-wave powers as a function of the cover-layer thickness, k_0t; $\varepsilon_r = 2.5$.

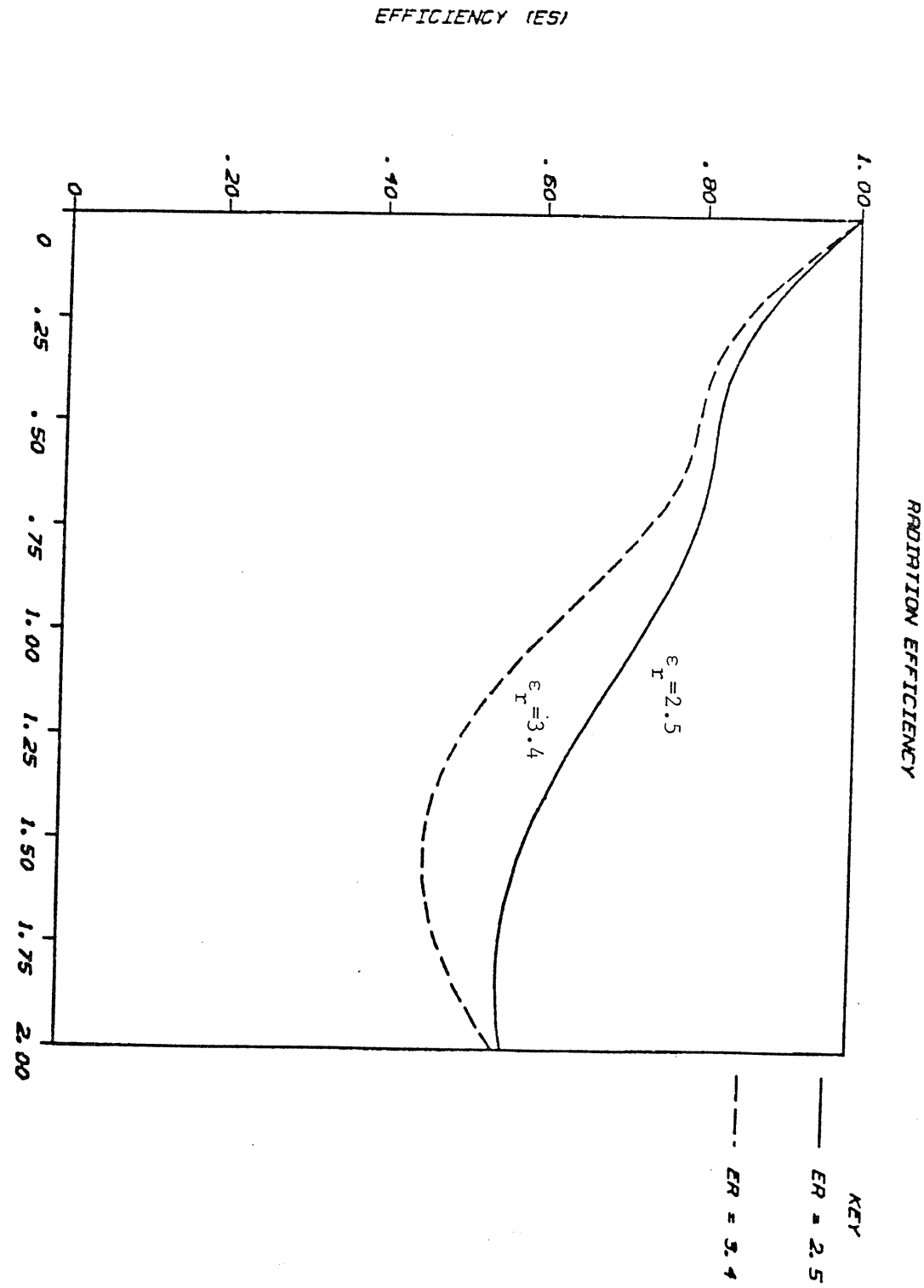

Fig. 7: The radiation efficiency, e_s, as a function of the cover-layer thickness, $k_0 t$; ε_r = 2.5 and 3.4.

5.2 Effects of Lossy Cover-Layer on Surface-Waves

In order to examine the effects of a lossy dielectric cover-layer on the surface-waves and the radiated power, in Figures 8 and 9, we have plotted P_{SW} (at $y = 1\ \lambda_0$) and P_r for a uniform lossy cover-layer. The results are shown for three different values of loss-tangent, $\tan\delta = 0.05$, 0.1 and 0.2. The results are normalized to the corresponding values of P_{SW} and P_r for the no-loss case (i.e., when $\tan\delta = 0.0$). As Figure 7 shows, at a lateral distance of one wavelength from the line-source (i.e., $\frac{y}{\lambda_0} = 1$), P_{SW} is attenuated between 4.5 and 6.5 dB, for $1 < k_0 t < 1.25$ and $\tan\delta = 0.2$. Also we note that, for the same parameters, the radiated power is reduced only by 2 dB, as shown in Figure 8. This means a net gain of 3 dB in reducing the surface-wave radiation as a side-lobe if the cover-layer is to be truncated at a distance of $y = 1\ \lambda_0$. As mentioned earlier, since the (TM_0) surface-wave is mainly contained inside the cover, in practice, one may use a graded lossy material instead of uniform loss, in order to cut down the surface-wave radiation and achieve better radiation characteristics.

6. Concluding Remarks and Discussions

A magnetic-current line source model has been used to analyze the radiation characteristics of a thin microstrip patch antenna with a dielectric cover-layer. Explicit expressions, showing the effect of the cover-layer thickness, have been derived for the far-field, radiated power, directivity and surface-wave power of the antenna. These are given by equations (20), (23), (27) and (34)-(39).

It has been found that the beamwidth of the radiation pattern in E-plane will initially decrease and then increase upon increasing $k_0 t$ (normalized thickness of the cover-layer). For small values of the cover-layer thickness, i.e., for $k_0 t << 1$, the (TM_0) surface-wave power, P_{SW}, is very small and consequently a radiation efficiency,

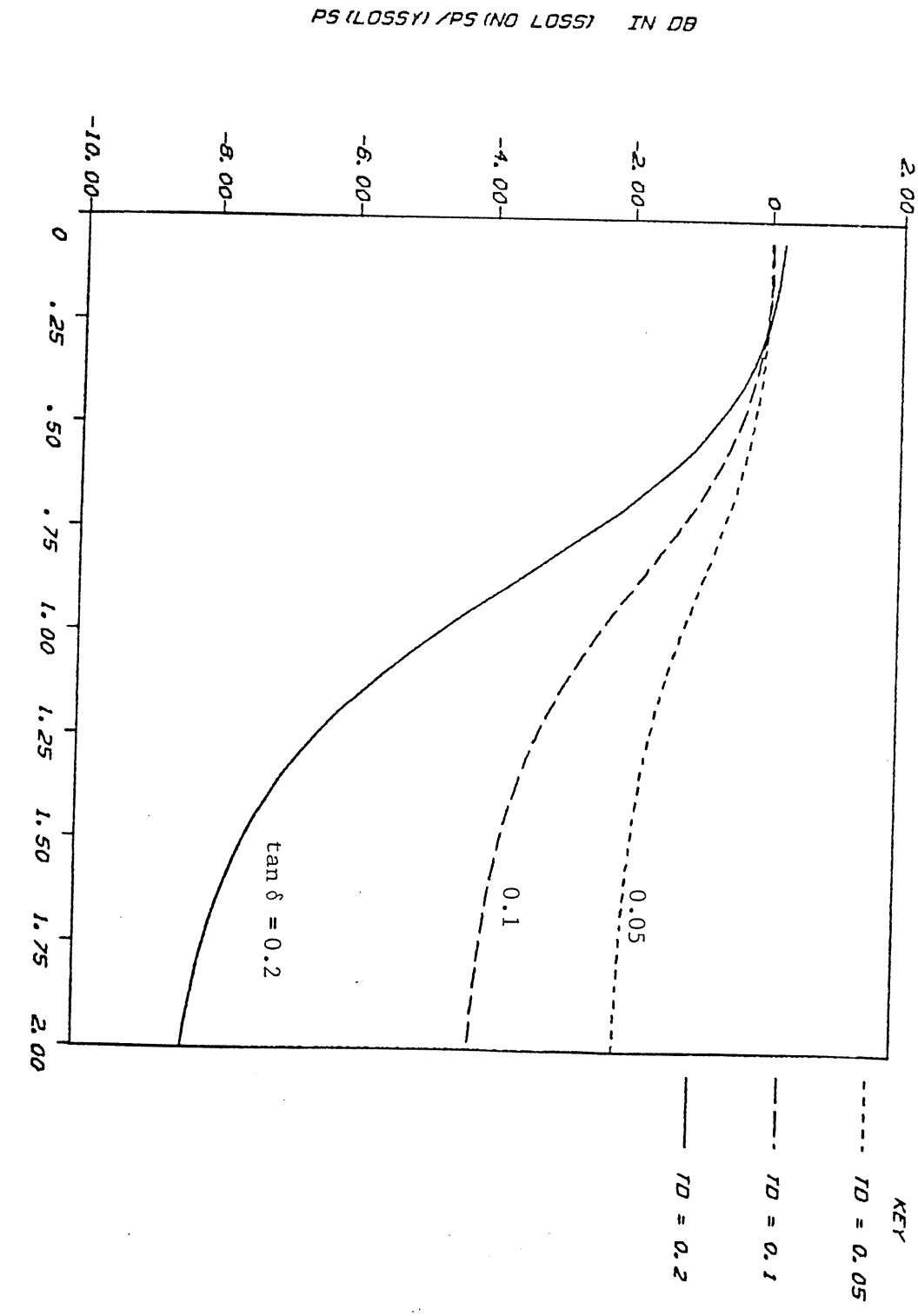

Fig. 8: Effects of a lossy cover-layer on the surface-wave power of a microstrip patch at a lateral distance of one wavelength from the edge (i.e., $y/\lambda_0=1$). The results are plotted for $\varepsilon_r = 2.5$ and for various values of dielectric loss-tangent.

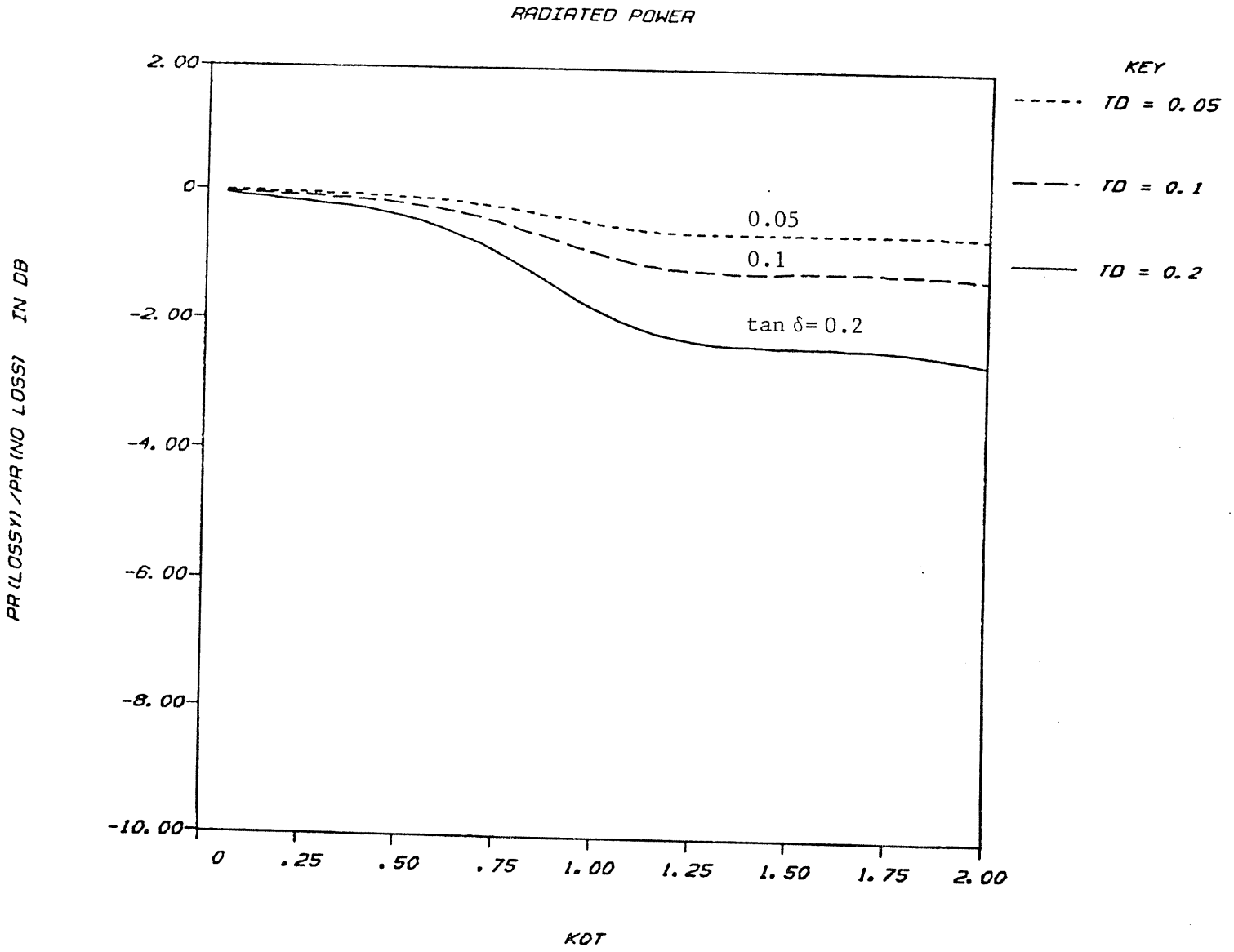

Fig. 9: Effects of a lossy cover-layer on the radiated power of a microstrip patch at a lateral distance of one wavelength from the edge (i.e., $y/\lambda_0 = 1$). The results are plotted for $\varepsilon_r = 2.5$ and for various values of dielectric loss-tangent.

e_s, of better than 90% can be achieved.

For large values of cover thickness, the surface-wave power is relatively large and the radiation efficiency is less than 70% for $k_0 t \geq 1$. It is interesting to note, however, that the power carried by the surface-wave is almost entirely contained inside the cover-layer. This suggests the possibility of using a lossy cover-layer in order to attenuate the surface-waves propagation, and their eventual radiation as a side lobe, for a finite-sized cover-layer. As the results in Figures 7 and 8 show, the surface-wave propagation can effectively be attenuated by using a lossy dielectric cover-layer. For example, for $\epsilon_r = 2.5$, and a uniform loss-tangent of 0.2, a net reduction of 3 dB or better in the surface-wave radiation can be achieved. Alternatively, one could use a graded lossy thin-film between the substrate and the cover-layer for attenuating the surface-waves.

The method used in this work for a semi-infinite patch can easily be extended to the case of a finite patch of length ℓ. The two radiating edges of the finite patch may be modeled by two magnetic-current line sources. The extension of the results in sections 3 and 4 to a two element line-source array is straightforward. In particular the TM_0 surface-wave field is given by

$$(E_z^a)_{SW} = (E_z)_{SW} \left(1 + e^{i\beta_p \ell}\right)$$

where $(E_z)_{SW}$ is derived in section 4. It is possible to eliminate the surface-wave, away from the radiating edges, i.e., for $y < 0$ and $y > \ell$, if we let $\beta_p \ell = \pi$. Also for the patch to be at resonance, we must have $k_s \ell \simeq \pi$ where k_s is the wave-number in the substrate. Therefore for the dominant TM_0 mode not to be propagated, one must have $\beta_p \simeq k_s$. Surprisingly, this condition is identical to that obtained by Alexopolous and Jackson [1], through a completely different physical argument in the analysis of a microstrip dipole antenna. As it is discussed in [1], however, this condition $\beta_p = k_s$

(together with the condition of all higher-order modes to be in "cut-off") requires the substrate to be extremely thin, unless a magnetic cover layer is used. Also, the design tends to be very narrow-band.

It should be noted that the formulation and results presented in this paper are accurately valid only when the (electrically thin) substrate is much thinner than the cover-layer. A more rigorous formulation for thicker substrate, based on the Wiener-Hopf technique, is in progress [9]. An initial comparison with the results in [9] shows that the present analysis could be used with an upper-bound error of less than 8% for $k_0 d < 0.13$ and $t/d > 4$.

References

[1] Alexopolous, N.G. and D.R. Jackson, "Fundamental superstrate (cover) effects on printed circuit antennas", *IEEE Trans. Ant. Prop.*, vol. AP-32, no. 8, pp. 807-816, August 1984.

[2] Hammer, P., D. Van Beauchante, D. Verschraven and A. Van De Capelie, "A model for calculating the radiation field of microstrip antennas", *IEEE Trans. Ant. Prop.*, vol. AP-27, no. 2, pp. 267-270, March 1979.

[3] Pues, H. and A. Van De Capelle, "Accurate transmission-line model for the rectangular microstrip antenna", *IEEE Proc.*, pt. H, pp. 334-340, 1984.

[4] Lo, Y.T., D. Solomon and W.F. Richards, "Theory and Experiment on Microstrip Antennas", *IEEE Trans. Ant. Prop.*, vol. AP-27, no. 2, pp. 137-145, March 1979.

[5] Harrington, R.F., *Time-Harmonic Electromagnetic Fields*, McGraw-Hill Book Company, 1961.

[6] Mosig, J.R. and F.E. Gardiol, "A dynamical radiation model for microstrip structures", *Advances in Electronics and Electron Physics*, vol. 59, pp. 139-237, 1982.

[7] Carver, K.R. and J.W. Mink, "Microstrip Antenna Technology", *IEEE Trans. Ant. Prop.*, vol. AP-29, no. 1, pp. 2-24, January 1981.

[8] Clemmow, P.C., *The Plane-Wave Spectrum Representation of Electromagnetic Fields*, Oxford: Pergamon Press, 1966.

[9] Tu, Y., K.C. Gupta and D.C. Chang, "Edge admittance for microstrip antennas with a dielectric cover layer", presented at the URSI Meeting, Boulder, Colorado, January 1986.